Angle-resolved phase-sensitive determination of the in-plane gap symmetry in $YBa_2Cu_3O_{7-\delta}$

J. R. KIRTLEY[1]*, C. C. TSUEI[1], A. ARIANDO[2], C. J. M. VERWIJS[2], S. HARKEMA[2] AND H. HILGENKAMP[2]

[1]IBM Watson Research Center, Route 134 Yorktown Heights, New York 10598, USA

[2]Faculty of Science and Technology and MESA+ Institute for Nanotechnology, University of Twente, PO Box 217, 7500 AE Enschede, The Netherlands

*e-mail: kirtley@us.ibm.com

Published online: 5 February 2006; doi:10.1038/nphys215

Understanding the nature of the ground state and its low-lying excitations in the copper oxide superconductors is a prerequisite for determining the origin of high-temperature superconductivity. A superconducting order parameter (that is, the energy gap) with a predominantly $d_{x^2-y^2}$ symmetry is well-established. However, various deviations from a pure d-wave pair state, such as the possibility of Cooper pairing with broken time-reversal symmetry or an admixed $d_{x^2-y^2}+s$ pair state, have been theoretically predicted and actively sought in numerous experimental studies. Here, we present an angle-resolved phase-sensitive technique for accurately determining the in-plane pairing symmetry, and demonstrate this technique in optimally doped $YBa_2Cu_3O_{7-\delta}$. We find that the gap along the b-axis (Cu–O chain) direction is at least 20% larger than that along the a-axis direction, and that any imaginary id_{xy}, is or ip component must be smaller than a few per cent of the $d_{x^2-y^2}$ component of the gap.

Phase-sensitive techniques for determining pairing symmetry have played a crucial role in settling the decade-long d-wave versus s-wave debate in favour of a gap with predominantly $d_{x^2-y^2}$ symmetry in various hole- and electron-doped cuprate superconductors[1–4]. There are, however, two important issues, the possibility of broken time-reversal symmetry (BTRS) and the size of the in-plane anisotropy in (for example) $YBa_2Cu_3O_{7-\delta}$ (YBCO), that remain highly controversial. BTRS has been suggested to occur either because of an intrinsic pairing process in the bulk[5,6] or extrinsically induced at surfaces or interfaces[7,8]. Although it is generally believed that there is little BTRS in optimally doped bulk cuprates[9,10], there have been reports of BTRS in the pseudogap state of underdoped cuprates from angle-resolved photoemission[11,12] and polarized elastic neutron diffraction[13], and several reports of evidence for BTRS in the cuprate superconductors from tunnelling measurements[14–16]. Many phase-sensitive experiments have sought evidence of BTRS[1,2,17,18], and concluded that, if present, it must be quite small for many cuprates and over a broad range of doping[4]. However, previous phase-sensitive measurements were made in a limited number of geometries. For example, a two-junction SQUID geometry in which the junction normals are perpendicular to the a- and b-axes[1] is insensitive to an imaginary d_{xy} component, which has nodes along the a- and b-axis directions. It is therefore important to perform phase-sensitive experiments as a function of in-plane momentum. Such experiments have been suggested to be sensitive to an imaginary component to the order parameter[19,20]. Another possible modification of the pure d-wave gap parameter is an admixed $d_{x^2-y^2}+s$ pair state, where s is the s-wave real component of the gap, as required by group theory for the in-plane Cu–O lattice symmetry of orthorhombic cuprate superconductors such as YBCO (ref. 2). Although a $d+s$ pair state in YBCO is established[21–26], reports of the magnitude of the s-wave admixture vary. Moreover, it is now established that, in cuprate superconductors, the low-temperature properties such as penetration depth and thermal conductivity are dominated by low-energy quasiparticle excitations across the nodes[27]. A precise knowledge of the momentum-dependent gap function in the vicinity of the nodes in the d-wave order parameter is important for understanding quasiparticle-related low-energy phenomena in HTS. Attempts at such experiments[28,29] have met with limited success.

The physics behind our experiment are well-established[2]. If there is an intrinsic phase shift of π between the phases of the normal components of the gap at the two junctions in a two-junction ring (π-ring), spontaneous supercurrents will circulate as the ring is cooled through the superconducting transition in zero field. Rings without such an intrinsic phase shift (0-rings) will not generate spontaneous supercurrents. In a π-ring with a sufficiently large product of the ring inductance L times the junction critical currents $I_{1,2}$, the spontaneously generated flux will be close to half of the superconducting flux quantum $\Phi_0 = h/2e$, where h is Planck's constant, if there is no imaginary component to the gap. However, if there is an imaginary component to the gap, the spontaneous flux will deviate from $\Phi_0/2$ or zero, depending on the details of the ring geometry.

We concentrate in this article on two samples. In these samples-72 rings are spaced by 400 μm in a square array. A schematic of a ring from sample 1 is shown in Fig. 1a. For this sample, each ring has one junction with a fixed angle of −22.5° relative to the majority twin a-axis direction in the YBCO, with the second junction angle varying in intervals of 5°. An optical micrograph of one ring is shown in Fig. 1b, and a scanning electron microscopy (SEM) image of one of the ramp-edge junctions is depicted in Fig. 1c. The ring geometries were optimized with several considerations in mind. For our measurements it is desirable to have large rings, because this leads to large I_cL products, so that the spontaneous magnetization is not reduced from the asymptotic $\Phi_0/2$ value. Large rings are also easier to resolve with the SQUID microscope. However, larger rings have smaller fields associated with a given flux, making precision measurements more difficult, and are also more likely to trap flux. It has been shown[30] that vortices are unlikely to be trapped in a superconducting line of width W if the ambient field is less than $B_x = \pi\Phi_0/4W^2$. For $W \sim 50$ μm, $B_x \sim 6.5 \times 10^{-7}$ T. We believe the ambient field during cooling was less than 10^{-7} T, from imaging the trapped vortices in large areas of superconducting films. There are no instances of vortices trapped in the ring walls or junctions in the data presented here. It is important that the junction interfaces are well-defined, clean and have a sufficiently high critical current density. We have been able to satisfy these conditions using a special fabrication process[31].

For the fabrication of the YBCO/Au/Nb ramp-edge Josephson junctions, first a 340 nm [001]-oriented YBCO and 70 nm $SrTiO_3$ (STO) bilayer is epitaxially grown by pulsed laser deposition (PLD). Then an array of YBCO semi-rings is defined using optical lithography and Ar-ion milling. The structures are carefully aligned with respect to the substrate main crystal axes. To ensure a well-defined ramp for all junction angles, the samples are at an angle of 45° with respect to the argon beam and rotated during Ar-ion milling. To enhance the transparency of the junctions, a 7 nm YBCO interlayer[31] is deposited, followed by the *in situ* PLD deposition of a 16 nm Au layer. The array of 160-nm Nb counter semi-rings is defined by optical lithography and sputtering using a lift-off mask. In the last step, the redundant uncovered YBCO/Au layer is removed by Ar-ion milling. A similar fabrication process was used to fabricate samples to measure the critical current as a function of junction angle[26]. As the experiments rely heavily on the asymmetry in the a- and b-axis directions of the YBCO, special care is taken to control the twinning. The films are grown on [100]-oriented single-crystalline STO substrates with a vicinal angle of ∼1° to obtain untwinned YBCO films[32]. X-ray diffraction

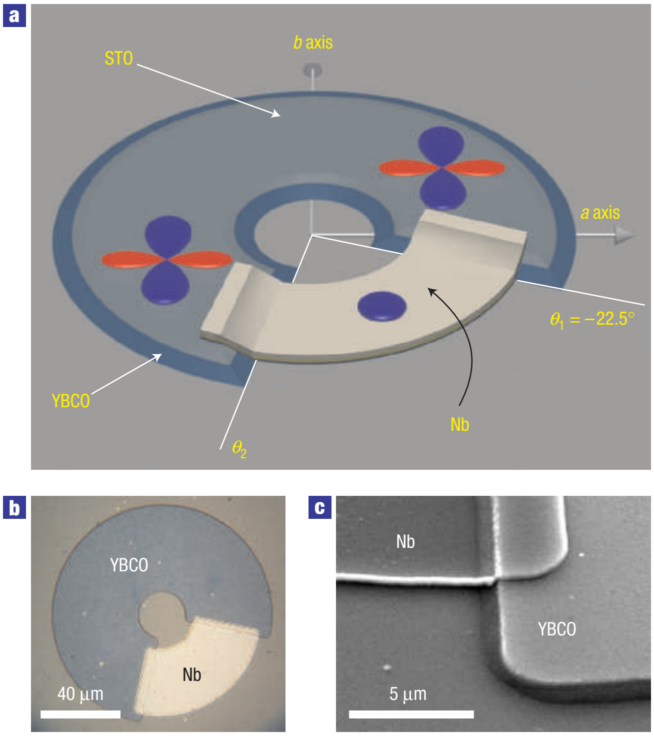

Figure 1 Experimental ring geometry. a, Schematic, **b**, optical micrograph and **c**, SEM micrograph of one of the rings of sample 1. In this sample, 72 rings were spaced by 400 μm on a square array, with the angles between the junction normals and the YBCO crystalline axes varying in 5° intervals. Each ring has a YBCO section with 15 μm (65 μm) inside (outside) radius, contacting a Nb section with 20 μm (60 μm) inside (outside) radius through two ramp-edge junctions. One junction normal angle was held fixed at −22.5° relative to the YBCO majority b-axis twin direction; the other was varied.

reciprocal space mapping confirmed that the YBCO films are highly untwinned (85% for both sample 1 and sample 2).

Our samples were imaged with a high-spatial-resolution scanning SQUID microscope[33]. Figure 2b shows a SQUID microscope image of one of the rings, cooled and imaged in zero field. The spontaneous flux is clearly visible in the centre of the ring; the ring walls are nearly invisible. Figure 2c shows images of the rings in this sample, cooled and imaged in zero field, depicted as a polar plot. This underlines the nearly four-fold symmetry of the data, with the transitions between 0-rings and π-rings occurring at angle of the variable junction normal $\theta = \theta_2 - 90°$ values close to $(2m+1)45°$, m being an integer. The deviations from four-fold symmetry are systematic and are consistent with the gap being larger in the b-axis direction than in the a-axis direction. The outer circle of images are of the sample cooled in zero field, in which case the rings either have zero spontaneous flux (fluxoid number $n = 0$) or spontaneous flux close to $\Phi_0/2$ ($n = 1/2$). To test whether all of the rings had sufficiently large junction critical currents to sustain an appreciable circulating supercurrent, we recooled the sample in a field of 0.2 μT, with the resulting images shown in the inner semi-circle of Fig. 2c. In this case the 0-rings were either in the $n = 1$ or 2 state, whereas the π-rings remained in the $n = 1/2$ state.

The solid points in Fig. 3 show the integrated flux in the rings of sample 1, cooled and imaged in zero field. This integration was done by first calculating the sum $\Sigma_s(A) = \sum_n \Phi_s(n)$ of the magnetic fluxes $\Phi_s(n)$ threading the SQUID pickup loop for

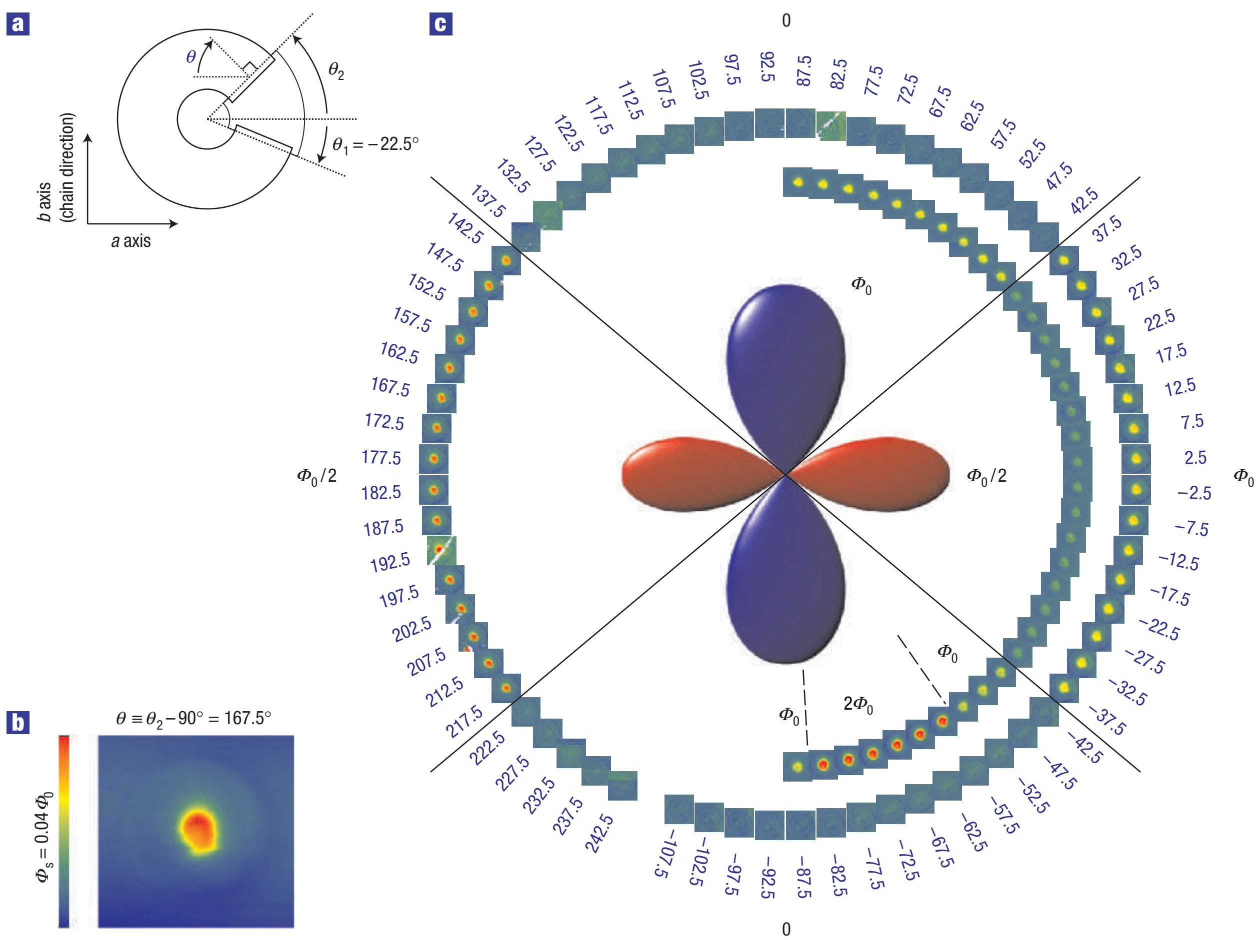

Figure 2 Schematic and SQUID microscope images of the rings of sample 1. a, Schematic of one ring, with the angles defined. **b**, An image of the ring with second junction normal angle $\theta = 167.5^\circ$ relative to the majority twin a-axis direction, cooled and imaged in nominally zero field. Each image, of a square area 150 μm on a side, was taken with a square pickup loop 8 μm on a side, with a calculated effective pickup area of 85.3 μm^2, at 4.2 K. **c**, Images for all of the rings in sample 1 labelled by θ and arranged in a polar plot. The outer circle of images, taken after cooling in zero field, has a full-scale variation of $0.04\,\Phi_0$ flux through the SQUID: the inner ring, taken after the sample was cooled in a field of 0.2 μT, has a full-scale variation of $0.09\,\Phi_0$. The rings cooled in zero field were either in the $n = 0$ or the $n = 1/2$ flux quantum states; the rings cooled in 0.2 μT were in the $n = 1/2$, $n = 1$ or $n = 2$ states.

all values of a circular integration area A. This sum is over all data elements with $r(n)$, the distance of the nth data element from the centre of the ring, less than R, with $A = \pi R^2$. With no background magnetic field, $\Sigma_s(A)$ should increase with A until $A = A_{\mathrm{min}}$, corresponding to the area of the inner diameter of the ring, and then be a constant proportional to the total magnetic flux threading the ring until $A = A_{\mathrm{max}}$, the area corresponding to the outer diameter of the ring, as the z-component of the field directly above the superconducting ring is zero. We compensate for constant offsets in the SQUID signal by fitting $\Sigma_s(A)$ to a straight line between A_{min} and A_{max}. After this linear background is subtracted from $\Sigma_s(A)$ to obtain $\Sigma_s^*(A)$, the total flux through the ring is $\Phi = A_{\mathrm{pixel}}\Sigma_s^*(A_0)/A_{\mathrm{loop}}$, where A_{pixel} is the area per data point (9 μm^2), A_{loop} is the effective area of the pickup loop (85.3 μm^2) and $\Sigma_s^*(A_0)$ can be evaluated at any value of A_0 between A_{min} and A_{max}, as by construction it is constant within experimental noise between these values. Here we used the conservative values $A_{\mathrm{min}} = 500$ μm^2 and $A_{\mathrm{max}} = 1{,}000$ μm^2 to allow for variations in the ring geometry and uncertainties in the ring positions. This method for determining the total flux in the rings is independent

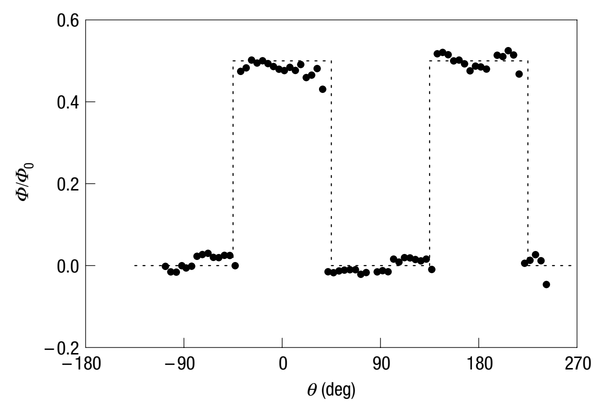

Figure 3 Integrated flux through the rings of sample 1, as a function of θ, the angle of the second junction normal relative to the majority twin a-axis direction. The solid points are the data, the dotted line is the expected dependence for a pure $d_{x^2-y^2}$ superconductor with $\beta \gg 1$.

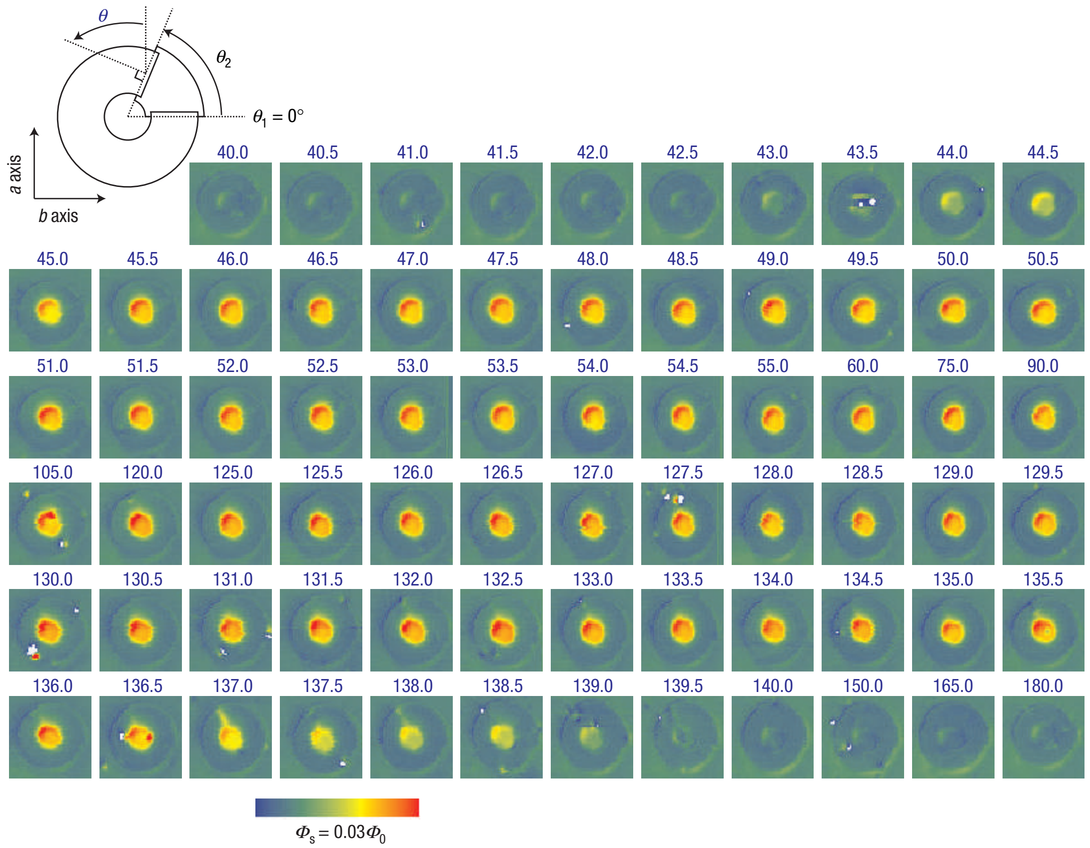

Figure 4 SQUID images of sample 2. The inset shows the ring geometry, which is the same as sample 1, except one junction normal is parallel to the majority twin a-axis, whereas the second has angle intervals of 0.5° in the nodal regions. The sample was cooled in zero field and imaged at 4.2 K with a square pickup loop 8 μm on a side. The images are labelled by θ, the angle of the variable junction normal relative to the majority twin a-axis.

of the height of the pickup loop above the sample surface within the parameter ranges used in our studies, does not depend on the details of the geometries of the rings, and produces values for the total flux from Abrikosov vortices trapped in bulk superconducting films in agreement with $\Phi = \Phi_0$ to within a few per cent[4]. The dotted line in Fig. 3 shows the expected behaviour for a pure $d_{x^2-y^2}$ pairing symmetry with a screening parameter $2\pi LI_{1,2}/\Phi_0 \gg 1$. The total flux in the π-rings is close to $\Phi_0/2$, whereas that in the 0-rings is close to zero. If we write the angular dependence of the YBCO gap as $\Delta(\theta) = \Delta_s + \Delta_{x^2-y^2}\cos(2\theta)$, where Δ_s is the s-component and $\Delta_{x^2-y^2}$ is the $d_{x^2-y^2}$ component of the in-plane gap, the node angle should satisfy $\theta_{\text{node}} = (1/2)\cos^{-1}(-\Delta_s/\Delta_{x^2-y^2})$. As the boundary between 0- and π-rings occurs between 37.5° and 42.5°, this implies that $-0.09 > \Delta_s/\Delta_{x^2-y^2} > -0.26$. This should be taken as an underestimate of the gap anisotropy, as twinning would tend to reduce the deviation of the nodal directions from $(2m+1)45°$. Measurements of the critical currents of single YBCO–Nb junctions made using the same technology, but with more highly untwinned YBCO films, resulted in a reported gap 50% larger in the b than the a direction[26].

Sample 2 was made with intervals of 0.5° in the second junction angle in the nodal regions. The results are summarized in Figs 4 and 5. In this case, the fixed junction had a normal parallel to the majority twin a-axis direction. The SQUID images in Fig. 4 show that spontaneous magnetization occurs for $43° < \theta < 139°$. Systematic transitions between no spontaneous flux and full $\Phi_0/2$ spontaneous flux are visible because of the small steps in θ. The solid points in Fig. 5 show the integrated flux from sample 2 cooled and imaged in zero field. The data have been shifted by $-1.5°$ along the θ axis, to correct for a small misalignment of the photolithographic mask with respect to the substrate crystalline axes, taking symmetry around $\theta = 90°$ as the criterion. The solid line in Fig. 5 is a fit to the data as follows: consider a two-junction ring with junction critical currents I_1 and I_2 and total inductance L, in zero field. The condition of a single-valued superconducting wavefunction leads to

$$\epsilon(\theta_1,\theta_2) - \sin^{-1}(I_s/I_1) - \sin^{-1}(I_s/I_2) - 2\pi LI_s/\Phi_0 = 2\pi n, \quad (1)$$

where $\epsilon(\theta_1,\theta_2)$ is the intrinsic phase drop in the YBCO between the two junctions in the absence of applied fields or supercurrents, $\theta_{1,2}$ are the angles of the two junctions relative to the YBCO crystalline axes, I_s is the supercurrent circulating around the ring, n is an integer and, assuming the standard Josephson current–phase relationship, $I_{s,1,2} = I_{1,2}\sin(\varphi_{1,2})$, where $\varphi_{1,2}$ are the quantum mechanical phase drops across the junctions. The intrinsic phase drop $\epsilon(\theta_1,\theta_2)$ around the ring can be considered as the sum of intrinsic phase drops $\epsilon_{1,2}$ across the individual junctions. If we write the component of the YBCO gap along the junction normal as $\Delta_{1,2} = \Delta_{r,1,2} + i\Delta_{i,1,2}$, then $\epsilon_{1,2} = \cos^{-1}(\Delta_{r,1,2}/\Delta_{t,1,2})$, where $\Delta_{t,1,2} = \sqrt{\Delta^2_{r,1,2} + \Delta^2_{i,1,2}}$. We assume the Sigrist–Rice form[34] for the junction critical currents: the critical currents are assumed to be proportional to the component of the YBCO gap normal to the junction. It is convenient to write the momentum-dependent gap

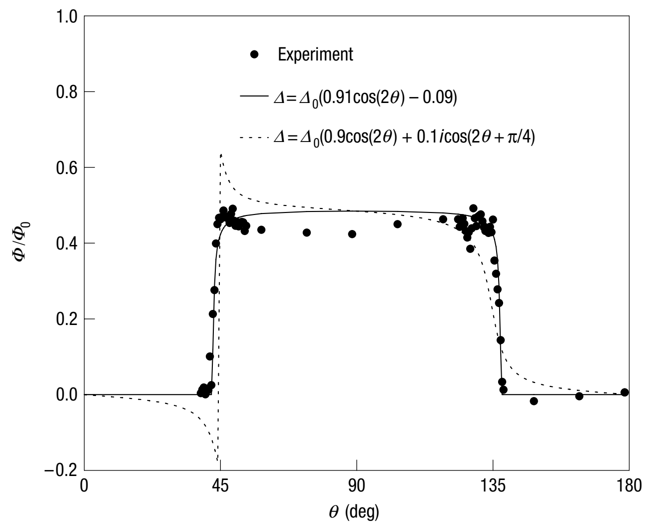

Figure 5 Integrated flux through the rings of sample 2, as a function of θ, the second junction normal angle relative to the majority twin *a*-axis direction. The solid points are the data; the solid line is a best fit to the model described in the text, with $\Delta(\theta) = \Delta_s + \Delta_{x^2-y^2}\cos(2\theta)$, allowing β and $\Delta_s/\Delta_{x^2-y^2}$ to vary. The best fit values were $\Delta_s/\Delta_{x^2-y^2} = -0.10 \pm 0.02$ and $40 < \beta < 150$. The dashed line shows the prediction for $\Delta(\theta) = \Delta_0(0.9\cos(2\theta) + 0.1i\cos(2\theta + \pi/4))$.

as $\Delta_{t,1,2}(\theta) = \Delta_0 F(\theta_{1,2})$ with $F(\theta = 0) = 1$. Then $I_{1,2} = I_0 F(\theta_{1,2})$. Equation (1) is solved for I_s for a given assumed functional form $F(\theta)$ for the gap at each angle: the total spontaneous flux through the ring is given by $\Phi = LI_s$. A fit between the resulting angle-dependent Φ_{theory} to the experimental Φ_{exp}, using the inductance-critical current product parameter $\beta = 2\pi LI_0/\Phi_0$ and $\Delta_s/\Delta_{x^2-y^2}$ as the two fitting parameters, gives $\Delta_s/\Delta_{x^2-y^2} = -0.10 \pm 0.02$ and $40 < \beta < 150$, using a doubling of the $\chi^2 = \sum_i (\Phi_{\text{exp}} - \Phi_{\text{theory}})^2$, where the sum i is over all of the rings, from its lowest value as a criterion for assigning parameter uncertainties. This best fit value for $\Delta_s/\Delta_{x^2-y^2}$ is within the allowed spread of values derived from sample 1 above. Measurements of control junctions with junction normals parallel to the YBCO crystalline axes and 40 μm lengths gave critical currents of around 2.5 mA. Combining this with our estimate of the ring inductance of about 55 pH gives $\beta \sim 400$, somewhat higher than our fit value. However, as indicated by the large errors, the fits are insensitive to the value of β for $\beta \gg 1$ and are highly sensitive to small systematic errors in the integration of the flux. The dashed line in Fig. 5 shows the results for a small imaginary d_{xy} component. Similar modelling sets upper limits of 2.5% on possible id_{xy} ($\sim\cos(2\theta + \pi/4)$), is or ip ($\sim\cos(\theta)$) components.

The experiments described above are the practical realizations of studies[19,20] aimed at quantifying deviations from a pure $d_{x^2-y^2}$ symmetry, in particular BTRS states. Our results show that the nodal direction in YBCO films with a predominant twin orientation is shifted by at least a few degrees from the $(2m+1)45°$ angles expected for a pure $d_{x^2-y^2}$ superconductor. From our measurements, the pairing symmetry in YBCO has $\Delta_s/\Delta_{x^2-y^2} \sim -0.1$, implying that the gap is at least 20% larger in the *b*-axis direction than in the *a*-axis direction, with imaginary d_{xy}, s or p components smaller than $0.025\Delta_{x^2-y^2}$. Our results show that the presence of the CuO chains along the b axis leads to a significantly larger gap as compared with the a-axis direction. Furthermore, our results underline the fact that BTRS is not associated with high-temperature superconductivity in optimally doped YBCO.

Received 10 November 2005; accepted 21 December 2005; published 5 February 2006.

References

1. van Harlingen, D. J. Phase-sensitive tests of the symmetry of the pairing state in the high-temperature superconductors-evidence for $d_{x^2-y^2}$ symmetry. *Rev. Mod. Phys.* **67,** 515–535 (1995).
2. Tsuei, C. C. & Kirtley, J. R. Pairing symmetry in cuprate superconductors. *Rev. Mod. Phys.* **72,** 969–1016 (2000).
3. Tsuei, C. C. & Kirtley, J. R. Phase-sensitive evidence for d-wave pairing symmetry in electron-doped cuprate superconductors. *Phys. Rev. Lett.* **85,** 182–185 (2000).
4. Tsuei, C. C. *et al.* Robust $d_{x^2-y^2}$ pairing symmetry in high-temperature superconductors. *Phys. Rev. Lett.* **93,** 187004 (2004).
5. Laughlin, R. B. The relationship between high-temperature superconductivity and the fractional quantum hall effect. *Science* **242,** 525–533 (1988).
6. Varma, C. M. Pseudogap phase and the quantum-critical point in copper-oxide metals. *Phys. Rev. Lett.* **83,** 3538–3541 (1999).
7. Sigrist, M. Time-reversal symmetry breaking states in high-temperature superconductors. *Prog. Theor. Phys.* **99,** 899–929 (1998).
8. Löfwander, T., Shumeiko, V. S. & Wendin, G. Andreev bound states in high-T_c superconducting junctions. *Supercond. Sci. Technol.* **14,** R53–R77 (2001).
9. Spielman, S. *et al.* Measurement of the spontaneous polar Kerr effect in $YBa_2Cu_3O_7$ and $Bi_2Sr_2CaCu_2O_8$. *Phys. Rev. Lett.* **68,** 3472–3475 (1992).
10. Lawrence, T. W., Szöker, A. & Laughlin, R. B. Absence of circular dichroism in high-temperature superconductors. *Phys. Rev. Lett.* **69,** 1439–1442 (1992).
11. Kaminski, A. *et al.* Spontaneous breaking of time reversal symmetry in the pseudogap state of a high-T_c superconductor. *Nature* **416,** 610–613 (2002).
12. Simon, M. E. & Varma, C. M. Detection and implications of a time-reversal breaking state in underdoped cuprates. *Phys. Rev. Lett.* **89,** 247003 (2002).
13. Fauqué, B. *et al.* Magnetic order in the pseudogap phase of high-T_c superconductors. Preprint at <http://arxiv.org/abs/cond-mat/0509210> 2005.
14. Covington, M. *et al.* Observation of surface-induced broken time-reversal symmetry in $YBa_2Cu_3O_7$ tunnel junctions. *Phys. Rev. Lett.* **79,** 277–280 (1997).
15. Dagan, Y. & Deutscher, G. Doping and magnetic field dependence of in-plane tunneling into $YBa_2Cu_3O_{7-x}$: possible evidence for the existence of a quantum critical point. *Phys. Rev. Lett.* **87,** 177004 (2001).
16. Sharoni, A. *et al.* Local and macroscopic tunneling spectroscopy of $Y_{1-x}Ca_xBa_2Cu_3O_{7-\delta}$ films: evidence for a doping-dependent *is* or id_{xy} component in the order parameter. *Phys. Rev. B* **65,** 134526 (2002).
17. Mathai, A., Gim, Y., Black, R. C., Amar, A. & Wellstood, F. C. Experimental proof of a time-reversal-invariant order parameter with a π shift in $YBa_2Cu_3O_{7-\delta}$. *Phys. Rev. Lett.* **74,** 4523–4526 (1995).
18. Schulz, R. R. *et al.* Design and realization of an all *d*-wave dc π-superconducting quantum interference device. *Appl. Phys. Lett.* **76,** 912–914 (2002).
19. Beasley, M. R., Lew, D. & Laughlin, R. B. Time-reversal symmetry breaking in superconductors: a proposed experimental test. *Phys. Rev. B* **49,** 12330–12332 (1994).
20. Ng, T.-K. & Varma, C. M. Experimental signatures of time-reversal-violating superconductors. *Phys. Rev. B* **70,** 054514 (2004).
21. Polturak, E., Koren, G., Cohen, D. & Aharoni, E. Measurements of the anisotropy and temperature dependence of the in-plane energy gap in $YBa_2Cu_3O_{7-\delta}$ using Andreev reflections. *Phys. Rev. B* **47,** 5270–5274 (1993).
22. Basov, D. N. *et al.* In-plane anisotropy of the penetration depth in $YBa_2Cu_3O_{7-x}$ and $YBa_2Cu_4O_8$ superconductors. *Phys. Rev. Lett.* **74,** 598–601 (1995).
23. Limonov, M. F., Rykov, A. I. & Tajima, S. Raman scattering study on fully oxygenated $YBa_2Cu_3O_7$ single crystals: *x*–*y* anisotropy in the superconductivity-induced effects. *Phys. Rev. Lett.* **80,** 825–828 (1998).
24. Lu, D. H. *et al.* Superconducting gap and strong in-plane anisotropy in untwinned $YBa_2Cu_3O_{7-\delta}$. *Phys. Rev. Lett.* **86,** 4370–4373 (2001).
25. Engelhardt, A., Dittmann, R. & Braginski, A. I. Subgap conductance features of $YBa_2Cu_3O_{7-\delta}$ edge Josephson junctions. *Phys. Rev. B* **59,** 3815–3822 (1999).
26. Smilde, H. J. H. *et al.* Admixtures to *d*-wave gap symmetry in untwinned $YBa_2Cu_3O_7$ superconducting films measured by angle-resolved electron tunneling. *Phys. Rev. Lett.* **95,** 257001 (2005).
27. Orenstein, J. & Millis, A. J. Advance in the physics of high-temperature superconductivity. *Science* **288,** 468–474 (2000).
28. Gim, Y., Mathai, A., Black, R., Amar, A. & Wellstood, F. C. Angular dependence of the symmetry of the order parameter in $YBa_2Cu_3O_{7-\delta}$. *IEEE Trans. Appl. Supercond.* **7,** 2331–2334 (1997).
29. van Harlingen, D. J., Hilliard, J. E., Plourde, B. L. T. & Yanoff, B. D. Extending SQUID interferometry beyond the cuprates and beyond d-wave symmetry. *Physica C* **317–318,** 410–420 (1999).
30. Clem, J. R. *American Physical Society, Annual March Meeting, 1998, Abstract K36.06* (American Physical Society, College Park, Maryland, 1998).
31. Smilde, H. J. H., Hilgenkamp, H., Rijnders, G., Rogalla, H. & Blank, D. H. A. Enhanced transparency ramp-type Josephson contacts through interlayer deposition. *Appl. Phys. Lett.* **80,** 4579–4581 (2002).
32. Dekkers, J. M. *et al.* Monocrystalline $YBa_2Cu_3O_{7-x}$ thin films on vicinal $SrTiO_3$ (001) substrates. *Appl. Phys. Lett.* **83,** 5199–5201 (2003).
33. Kirtley, J. R. *et al.* High-resolution integrated scanning SQUID microscope. *Appl. Phys. Lett.* **66,** 1138–1140 (1995).
34. Sigrist, M. & Rice, T. M. Paramagnetic effect in high-T_c superconductors-a hint for *d*-wave superconductivity. *J. Phys. Soc. Jpn* **61,** 4283–4286 (1992).

Acknowledgements

We would like to thank D. Blank, A. Brinkman, M. Dekkers, A. Golubov, R. Koch, D. Newns, G. Rijnders, F. Roesthuis, H. Rogalla, H.-J. Smilde and C. Varma for discussions. This work was supported by the Dutch Foundation for Research on Matter (FOM), the Netherlands Organization for Scientific Research (NWO), the Dutch STW NanoNed programme, the European Science Foundation (ESF) PiShift programme, and by the Center for Probing the Nanoscale (CPN), an NSF NSEC, NSF Grant No. PHY-0425897.
Correspondence and requests for materials should be addressed to J.R.K.

Competing financial interests

The authors declare that they have no competing financial interests.